Synthesis of gold, silver and their alloy nanoparticles using bovine serum albumin as foaming and stabilizing agent†

Ajay V. Singh, Bapurao M. Bandgar, Manasi Kasture, B. L. V. Prasad* and Murali Sastry‡*

Received 20th July 2005, Accepted 27th September 2005
First published as an Advance Article on the web 18th October 2005
DOI: 10.1039/b510398c

A simple and convenient method for the synthesis of gold, silver and their alloy nanoparticles in a foam matrix using the protein bovine serum albumin (BSA) is reported. BSA is an excellent foaming agent and,by virtue of its zwitterionic character at the protein isoelectric point, may be used to bind to either cationic silver (Ag^+) or anionic gold ($AuCl_4^-$) ions in the foam. The metal ions in the foam are thereafter reduced *in situ* to yield silver and gold nanoparticles. The versatility of an amphoteric foaming agent is further demonstrated by the simultaneous binding of Ag^+ and $AuCl_4^-$ ions with zwitterionic BSA leading to the possibility of obtaining Au–Ag alloy nanoparticles in the foam. The BSA molecules coat and stabilize the nanoparticles thus prepared eliminating the necessity of employing an additional stabilizing agent in the experimental recipe.

Introduction

Investigations on different preparation techniques for obtaining materials at the nanometer level constitute a major area of research today. Fundamentally new properties and functions are expected from these materials resulting from their small sizes and modified electronic structures.[1] Among the perceived applications of these materials, much current interest is centered on applications related to biological processes such as drug delivery, biodiagnostics, *etc*.[2] Consequently, one of the challenges in nanomaterial synthesis is developing methodologies with biological molecules as templates for nanomaterial synthesis.

Apart from the synthesis of individual metal nanoparticles, composite materials like alloys and core–shell structures have also been the focus of research lately.[3] The interest in these structures stems from the unusual properties they are expected to show including superior opto-electronic properties[4] and better catalytic properties[5] than the individual metal nanoparticles. Many preparation techniques have already been reported to produce Au–Ag composite nanoparticles; however, relatively few methods produce alloy nanoparticles instead of core–shell particles, due to phase separation.[6] The alloy formation can easily be seen by a linear dependence of the plasmon absorption maximum with respect to the composition of Au *vs.* Ag in the alloy nanoparticles.[6f] However, many of the alloy preparations are still beset with certain issues that are ambiguous. For example, in cases where citrate reduction of Au–Ag salt mixtures is used for alloy formation, it is not clear how silver is incorporated into the alloy phase when silver alone is not easily reduced by sodium citrate.[6f] A possibility is that a catalytic process is operative where silver can be reduced only in the presence of gold nanoparticles, thus facilitating alloy formation.[6h] In many other cases where a surfactant is used in the preparation procedure, the surfactant may preferentially bind to oppositely charged ions due to electrostatic considerations, thus resulting in phase separation. Therefore, any efforts to make large quantities of alloy materials using these methods could lead to difficulties with respect to phase-pure formation of alloy nanoparticles.

While on the look-out for novel water-based methods for the synthesis of nanomaterials, we have identified aqueous foams as an excellent template for the growth of nanoparticles over a range of chemical compositions. There have been many reports on the synthesis of nanomaterials in restricted spaces and interfaces such as the air/water interface, liquid/liquid interface and in thermally evaporated thin films, *etc*.[7] In many ways liquid foams also possess similar interfaces and also provide an extremely large interfacial area crowded with surfactant molecules, which are basically amphiphiles that assemble at the gas/liquid interface. These essentially form extended monolayers akin to Langmuir monolayers juxtaposed on one another in a region of water with the polar groups facing each other,[8] providing us a template that could be used for material synthesis. Except in the report of Davey and co-workers,[9] who have used foams as templates for the nucleation of calcium carbonate, carrying out *in situ* chemical reactions in foams as a means of synthesis of nanomaterials is not well known. Some of us have recently used the foam-template for synthesis of various metal nanoparticles,[10] minerals[11] and oxide[11] nanoparticles. Surfactants such as sodium dodecyl sulfate (SDS), sodium bis(2-ethylhexyl)sulfosuccinate (AOT) and cetyltrimethylammonium bromide (CTAB) are popular choices for use as foaming surfactants and based on the charge of the metal ion, an oppositely

Nanoscience Group, Materials Chemistry Division, National Chemical Laboratory, Pune – 411 008, India. E-mail: pl.bhagavatula@ncl.res.in; m.sastry@ncl.res.in; Fax: +91 20 25893952/25893044; Tel: +91 20 25893044

† Electronic supplementary information (ESI) available: UV-Vis spectra obtained from the nanoparticles dispersion prepared in the control experiments, i) when the foam is formed from a 3 : 1 molar mixture of $HAuCl_4$ and Ag_2SO_4 with CTAB (Fig. S1) and ii) when the reduction is carried in a solution mixture of $3AuCl_4^-$: $1Ag^+$: BSA (Fig. S2). See DOI: 10.1039/b510398c

‡ Current address: Tata Chemicals Limited, Mumbai 400 059, India. E-mail: msastry@tatachemicals.com

charged surfactant is selected to enable electrostatic complexation between the two.

Once the foam is formed, the preparation of simple metals, semiconductors, minerals and metal oxide nanoparticles containing a single metal is rather straightforward.[10–12] On the other hand, preparing composite materials such as alloys using foams, especially when the metal ions possess opposite charges, is a non-trivial experimental problem. In this context, amphoteric molecules such as proteins would come in handy—at the isoelectric point, the zwitterionic proteins could bind simultaneously to cationic and anionic metal complexes. Bovine serum albumin (BSA) is an ideal candidate for this application since it shows excellent foaming behavior[13–15] in addition to the amphotericity mentioned above. In this paper, we demonstrate that versatile BSA may be used to either bind separately with aqueous Ag^+ or $AuCl_4^-$ ions at the isoelectric point, pI, of the protein (BSA pI = 4.7) or with both ions simultaneously at the pI. Formation of foam followed by *in situ* reduction of the ions in the foam results in the formation of pure Ag and Au nanoparticles as well as their alloys. The proximity of the silver and gold ions by virtue of the fact that they are complexed with the zwitterionic protein molecules is expected to facilitate the formation of the alloy phase over the pure metal phase. Here, the foaming step makes sure that only ions bound to BSA and thus in close propinquity with each other are reduced facilitating the alloy formation. In contrast the reduction in solution is indiscriminative and was found to result in the formation of separate nanoparticles of gold and silver along with a small portion of alloy phase (*vide infra*).

The BSA foam procedure also results in the nanoparticles being coated/stabilized by the BSA molecules. Many interesting reports have appeared in the literature where polypeptides/proteins have been used to assemble nanoparticles[16] or the nanoparticle surfaces have been modified by protein/polymer coatings[17] owing to their interest in the field of biomedical applications.[18] However, in most of these cases the assembly or modification of the surface is done on preformed nanoparticles. In our experiments the protein is used as a template to synthesize the nanoparticles. This could probably lead to a better coverage of the nanoparticles surface with the protein making them a better candidate for biological applications. Presented below are the details of the investigation.

Experimental

Chemicals

Hydrochloroauric acid ($HAuCl_4$), silver sulfate (Ag_2SO_4), bovine serum albumin (BSA), cetyltrimethylammonium bromide (CTAB) and hydrazine monohydrate ($N_2H_4{\cdot}H_2O$) were obtained from Aldrich Chemicals and used as-received.

The complete details of the foam experiments have been presented in the earlier papers[10b,11] and only a brief description relevant to the current investigation is provided here. In a typical experiment, a rectangular perspex column of 50 cm height and a square base of 10 × 10 cm^2 with a sintered frit embedded at the bottom was used for foam generation. For the synthesis of Ag and Au nanoparticles (NPs), 50 ml aqueous solution of BSA of concentration 3 mg ml^{-1} and 50 ml of $HAuCl_4$ or Ag_2SO_4 of 1 × 10^{-3} M concentration were taken separately and mixed with the BSA solution; the pH of this mixture (and in all other experiments discussed subsequently) was adjusted to 4.7 to be close to the pI of BSA. A foam was generated by passing nitrogen gas through the frit fitted at the base of the column. Stable foams of up to 40 cm height could be obtained quite easily. Thereafter, the gas flow was stopped and the excess liquid was allowed to drain out under gravity for 15 min. The reduction of the metal ions *in situ* was carried out by passing hydrazine hydrate vapors through the dry foam for 1.5 hours, this process leading to a dramatic appearance of color in the foam. The Ag and Au NPs were collected in solution form by spraying distilled water from the top of the foam column. For the synthesis of Au–Ag alloy nanoparticles a similar foam experiment to the one described above was performed, but by taking mixtures of Ag_2SO_4 and $HAuCl_4$ solutions together with BSA to prepare the foam. Systematic experiments were carried out by varying the molar ratios of Ag^+ and $AuCl_4^-$ in the mixture, in order to find out the best conditions for alloy formation. In the first experiment, 50 ml aqueous solution of 3 mg ml^{-1} BSA was mixed with 25 ml each of 1 × 10^{-3} M aqueous solutions of $HAuCl_4$ and Ag_2SO_4 and the foam generated metal ions reduced as mentioned above (1Au : 1Ag). The experiments were repeated by taking mixtures of 25 ml each of 1 × 10^{-3} M of $HAuCl_4$ and 3 × 10^{-3} M Ag_2SO_4 with 50 ml of 3 mg ml^{-1} BSA (1Au : 3Ag), or 3 × 10^{-3} M $HAuCl_4$ and 1 × 10^{-3} M Ag_2SO_4 with BSA (3Au : 1Ag). It was observed that better alloy nanoparticles formed with a 3Au : 1Ag mixture (*vide infra*). The reduced Au–Ag alloy nanoparticles were collected by spraying distilled water from the top of the foam column. The collected solutions were centrifuged at 10000 rpm for 15 minutes. The pellets were washed with distilled water and were subjected to centrifuging again. This process was repeated thrice and the final pellet samples were taken for the further characterization by UV-visible spectroscopy and transmission electron microscopy.

The two main aspects of the present paper, that zwitterionic surfactant BSA and its foaming nature are indeed necessary to obtain the alloy nanoparticles, were confirmed by doing the following control experiments. In the first control experiment the molar concentrations Ag_2SO_4 and $HAuCl_4$ were kept same as in the alloy formation experiment (3Au : 1Ag) described above. 25 ml each of 3 × 10^{-3} M $HAuCl_4$ and 1 × 10^{-3} M Ag_2SO_4 were mixed with 50 ml of 2 × 10^{-2} M solution of CTAB (a cationic surfactant and therefore capable of binding only to $AuCl_4^-$ ions). A foam was generated exactly as described above and the excess liquid was allowed to drain out. After waiting for 30 min, the foam was exposed to hydrazine hydrate vapors for 1.5 hours. The foam changed color from pale yellow to deep pink. The NPs generated in this foam were collected in solution form by spraying water and the obtained solutions were subjected to UV-Vis spectroscopic analysis. A single strong peak centered around 545 nm was observed indicating that only gold nanoparticles are formed in this experiment.

In the second control experiment, which was done to highlight the importance of the foaming step, 25 ml each of 3 × 10^{-3} M $HAuCl_4$ and 1 × 10^{-3} M Ag_2SO_4 aqueous solutions were mixed with 50 ml of 3 mg ml^{-1} BSA–water in a beaker. This mixture was then exposed to hydrazine hydrate vapors by

placing a beaker containing this mixture in a larger beaker containing the hydrazine hydrate solution and isolating the whole system from the surroundings. Please note that no foam was generated in this control experiment. UV-Vis spectroscopic analysis of the mixture after several hours of exposure clearly revealed two distinct peaks corresponding to the formation of silver and gold nanoparticles separately.

Atomic absorption spectroscopy (AAS) measurements were also done both on solution samples and also on dry foam samples of the above two mixtures before the reduction step was carried out. From these results we could estimate the different binding capacities of CTAB and BSA with $AuCl_4^-$ and Ag^+ ions and thus were able determine the relative ratios of these ions in solution and in foam in a quantitative manner.

FTIR measurements

FTIR measurements were carried out on a Perkin Elmer Spectrum-One spectrometer operated at a resolution of 4 cm^{-1}. For FTIR spectroscopy measurements foams were generated from 25 ml each of 3×10^{-3} M $HAuCl_4$ and 1×10^{-3} M Ag_2SO_4 aqueous solutions mixed either individually or together with 50 ml of 3 mg ml^{-1} BSA–water. After the dry foams were formed few bubbles were disrupted and the powders were collected. These were mixed with KBr and the FTIR measurements were carried out.

UV-Vis spectroscopy studies

The optical properties of gold, silver and gold-silver alloy nanoparticles at various metal salt concentrations were monitored on a Jasco UV-Vis spectrophotometer (V570 UV-VIS-NIR) operated at a resolution of 2 nm.

TEM measurements

TEM samples of gold, silver and Au–Ag alloy NPs synthesized in the foam were prepared by placing a few drops of the aqueous dispersions over carbon coated copper grids and allowing them to dry. TEM measurements were performed on a JEOL model 1200EX instrument operated at an accelerating voltage of 80 kV.

Results and discussion

BSA is one of the most widely studied proteins and is the most abundant in plasma with a typical concentration of 5 mg per 100 ml. It possesses a zwitterionic character at the isoelectric point (pI 4.7) with exposed ionic groups (C and N terminus) at the side chains of the globular protein, which are present in solution and are promising sites for binding cationic and anionic groups.[13] Apart from attributes like lowering of surface tension, foaming in proteins is also influenced to a great extent by the capacity to form semi-solid films at the air/solution interface assisted by the denaturation of the polypeptide chains and unfolding of the protein.[14] It is explained that this condition is greatly fulfilled at the pI of the protein due to the presence of minimum net charge on the protein and hence a maximum propensity to form the foam. Two parameters i) foam expansion index (FEI), and ii) foam liquid stability (FLS) are normally referred to for two distinct stages of foams, namely, formation and stability.[15] Here, higher numbers of these two parameters are attributed to greater foam forming ability and greater stability of the foam, respectively. For BSA the numbers are 280% (FEI) and 12% (FLS) as compared to 0% and 0% for lysozyme and 240% and 24% for egg albumen.[15] Consequently, the positively charged lysozyme, though known to play a vital role in the stability of egg albumen foams, by itself does not form good foams.[14d] On the other hand the foaming capacity of egg albumens is not as good as BSA but they have a better stability than BSA foams. It is also to be noted that these numbers might change in the presence of metal ions; it is not in the purview of this paper to study the formation/stability of the foams with different proteins *vis-à-vis* different metal ions. In any case, for our experiments we found that BSA forms excellent and stable foams and all the experiments were thus performed with BSA.

The general process for the synthesis of nanomaterials in a foam matrix involves the electrostatic complexation of metal ions with oppositely charged surfactant molecules, followed by the foam generation and subsequent *in situ* chemical reaction appropriate for the desired material.[10–12] As mentioned previously, BSA imparts greater flexibility to this method by allowing complexation of metal ions with opposite charges simultaneously. Indeed, we found that stable foams could be obtained when both Ag^+ and $AuCl_4^-$ ions are taken separately or simultaneously in the BSA–water mixture. Immediately after the foam is formed, there is a large excess of liquid in the foam column. This excess liquid is allowed to drain out to result in what is called a dry foam. In this situation the liquid volume fraction is expected to be at the minimum (in the ideal case) and the bubbles in the foam assume polyhedral shapes and the liquid lamellae between the faces of the bubbles are very thin. Since the BSA is now at the pI the availability of exposed ionic groups (C and N terminus) is maximum and it should allow large complexation of metal ions into the foam matrix. From the protein structure of serum albumins it can be found easily that the ionic groups are spatially well spread across the protein molecule and hence should allow the proximity for $AuCl_4^-$ and Ag^+ ions, when taken together, necessary for the formation of alloy nanoparticles.[19]

The formation of the metal nanoparticles can be easily proved by the combination of optical absorption studies, transmission electron microscopy (TEM) and selected area diffraction pattern analysis. In Fig. 1A and B, representative TEM images recorded from drop-coated films of the gold NPs prepared by the reduction of $AuCl_4^-$ ions in BSA foam by hydrazine are shown. The particles are polydisperse in nature with an average size of 30–60 nm. However, few particles tend to form irregular aggregates, which are seen as larger particles on the TEM image (Fig. 1B). The inset in Fig. 1B shows the selected area electron diffraction (SAED) pattern of the gold nanoparticles and can be indexed to the 111, 200, 220, 311 Bragg reflections appearing from the fcc gold structure. The TEM micrographs for silver nanoparticles synthesized in similar conditions to those described for gold nanoparticles are shown in Fig. 1C and D. The nanoparticles are predominantly spherical in shape and polydisperse with diameters in the range 20–80 nm. The inset of Fig. 1D show the SAED for silver NPs and the ring pattern is indexed to the

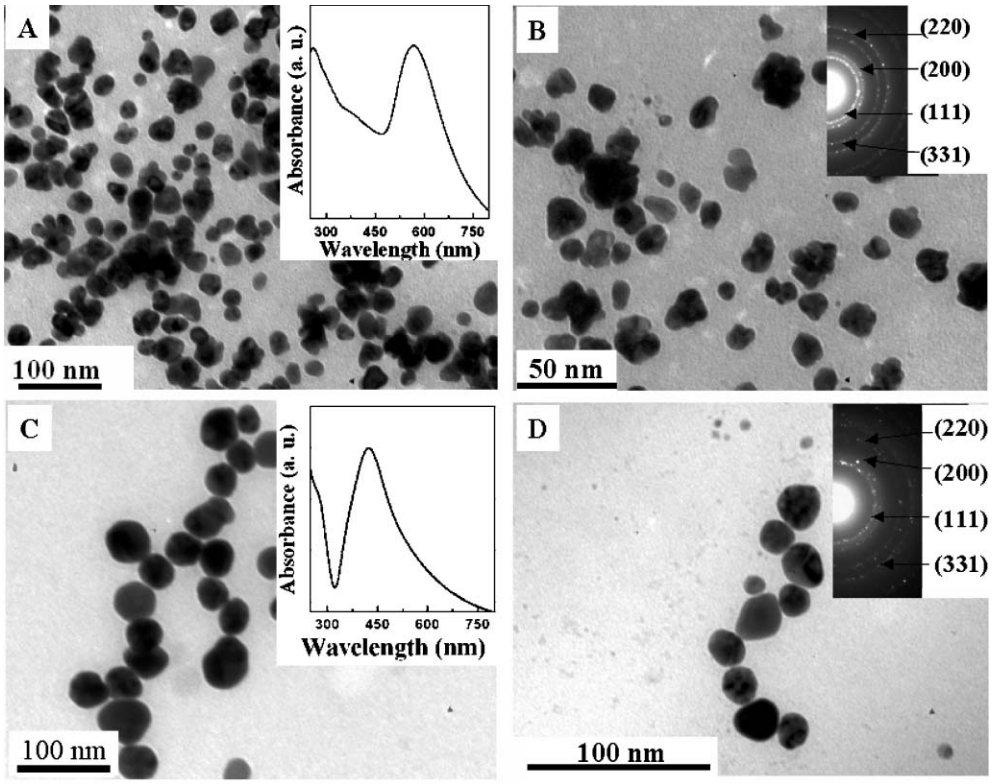

Fig. 1 (A, B) Representative TEM micrographs obtained from drop-coated films of Au nanoparticles prepared in the BSA foam. The inset in A shows the UV-Vis absorption spectrum of Au NPs. The inset in B shows the SAED pattern recorded from the Au nanoparticles. (C, D) Representative TEM micrographs obtained from a drop-coated film of Ag NPs prepared in the BSA foam. The inset in C shows the UV-Vis absorption spectrum of the Ag NP sol. The inset in D corresponds to the SAED of the silver nanoparticles.

111, 200, 220 and 311 Bragg reflections from the fcc structure of silver.

It is well known that silver and gold nanoparticles exhibit yellowish-brown and violet colors respectively in aqueous solution, these colors arising due to excitation of surface plasmon vibrations in the metal nanoparticles.[4] The insets in Fig. 1A and C show the UV-Vis spectra for gold and silver nanoparticles synthesized by hydrazine reduction in BSA foam. The absorption bands at 570 nm and 429 nm correspond to the surface plasmon excitations in gold and silver nanoparticles respectively. The peak positions in each case correspond to particles with sizes <100 nm,[20] which is also confirmed from the TEM micrographs obtained. The bright colors of the aqueous Au and Ag nanoparticle solutions obtained in the BSA foam are clearly seen in the images of test tubes 1 and 3 bearing these solutions respectively (inset, Fig. 2B). Thus, it is clear that one can obtain gold and silver nanoparticles using BSA as a foaming agent. This is the first report where nanoparticles of Ag and Au from Ag^+ and $AuCl_4^-$ ions are prepared using the same foaming surfactant; normally, an oppositely charged surfactant would have to be used depending on the nature of the metal ion to be complexed (*e.g.*, cationic CTAB with $AuCl_4^-$ and anionic SDS with Ag^+ ions). This unique property where the same surfactant is able to bind to two oppositely charged ions is further used to bind them simultaneously to the protein at its pI for the synthesis of Au–Ag alloy NPs and is discussed further.

Fig. 2 shows the UV-vis spectra of the BSA-capped gold, silver and gold–silver alloy nanoparticles in solution obtained from the mixtures of different molar ratio solutions of Ag^+ and $AuCl_4^-$. Curve 1 in Fig. 2A corresponds to the optical absorption spectrum obtained from a dispersion prepared from the mixture of 1Au : 3Ag foam. Curve 2 is the same obtained from 1Au : 1Ag and curve 3 is from 3Au : 1Ag. In Au–Ag alloy nanoparticles it is reported that a linear dependence of the plasmon absorption maximum on the composition of the nanoparticles can be found.[5f] As mentioned earlier individual silver and gold nanoparticles prepared under similar conditions absorb around 429 nm and 570 nm, respectively. Therefore, it is expected that alloy nanoparticles with 50 : 50 composition will have optical absorbance between these two. It is clear from Fig. 2A that only in the case of 3Au : 1Ag mixture, an appreciable shift in the optical absorbance.(a peak centered at $\sim$495 nm) is seen. In Fig. 2B we display the optical absorbance of individual nanoparticles of Ag (curve 1) and Au (curve 3) overlaid with that of the alloy nanoparticles obtained with a 3Au : 1Ag mixture (curve 2). The alloy formation may be concluded from the distinctly different colour of the solution as shown in the photograph of the test tube containing this solution (test tube no. 2, inset Fig. 2B) and the fact that the optical absorption spectrum shows only one plasmon band nearly at the center of the peaks corresponding to individual silver and gold nanoparticles. Two bands would be expected for the case of a mixture of gold and silver nanoparticles as well as for core–shell NPs.[6d] Here, we

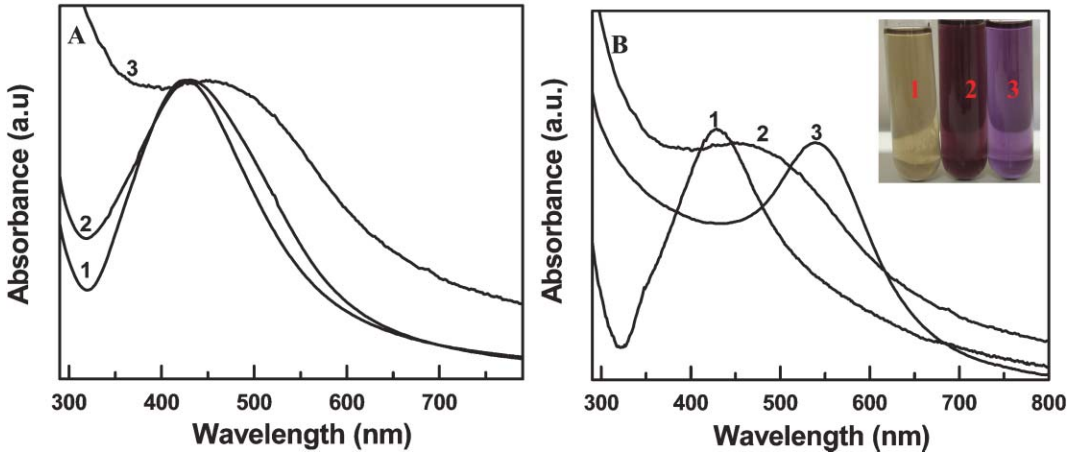

Fig. 2 A) UV-Vis absorption spectra recorded from nanoparticles obtained in the BSA foam experiment from (1) 1Au : 3Ag mixture; (2) 1Au : 1Ag mixture and (3) 3Au : 1Ag mixture. (B) UV-Vis absorption spectra recorded from (1) BSA-capped Ag NP solution, (2) BSA-capped Au–Ag alloy NP solution obtained from 3Au : 1Ag mixture and (3) BSA-capped Au NP solution. Photograph of the three test tubes with aqueous solutions of Ag, Au–Ag alloy and Au NPs, respectively, is shown in the inset of B.

would like to emphasize again that when we did the reduction of a 3Au : 1Ag : BSA mixture in solution we could observe two distinct peaks attributable to separate Ag and Au nanoparticles clearly establishing the necessity of the foaming step. At this time it is unclear why we are observing alloy nanoparticle formation only when we have excess $AuCl_4^-$ ions. It is well known that in the deposition of bulk alloys several different parameters including the nature of metal complexes being used, the ratios of metal ion concentrations and pH apart from the differences in their redox potentials as well as the differences in the activity coefficients of the two ions play a crucial role.[21] Several of these factors separately or in tandem could be contributing to this particular feature that we require an excess of $AuCl_4^-$ ions with respect to Ag^+ ions in the foam to get a good alloy composition. We are currently undertaking further studies especially involving other foaming proteins to understand this effect more clearly.

Transmission electron microscopy was utilized to analyze the size and protein coating of the alloy nanoparticles. Fig. 3A, B show the TEM micrographs recorded at different magnification from a drop cast film of BSA capped Au–Ag alloy NPs obtained in the 3Au : 1Ag experiment. The size of alloy NPs varies from 5–15 nm and they are spherical in shape. It is interesting to note that a fairly well defined inter-particle separation exists in the assemblies and they are not in direct physical contact. This provides the evidence for a protective BSA protein sheath around the alloyed NPs. The selected area electron diffraction (SAED) pattern is shown in Fig. 3B, confirming that the NPs formed are crystalline in nature belonging to a fcc lattice. Both Au and Ag adopt a fcc structure and have very close crystal lattice parameters. Hence it would be very difficult to observe any shifts in the positions of the rings from those of individual Au or Ag nanoparticles.

Two control experiments were done in order to ascertain beyond doubt that BSA and foaming are indeed necessary to obtain the alloy nanoparticles. In the first control experiment where we mimic the 3Au : 1Ag experimental conditions of the above procedure but replace BSA with CTAB, we got only gold nanoparticles showing a characteristic optical absorption at ~545 nm (see ESI,† Fig. S1). This is in concurrence with the expectation that CTAB being a positively charged surfactant would only bind to $AuCl_4^-$ ions thus carrying only those into the foam matrix. Data from the atomic absorption spectroscopy (AAS) studies also confirm this. Typically, AAS

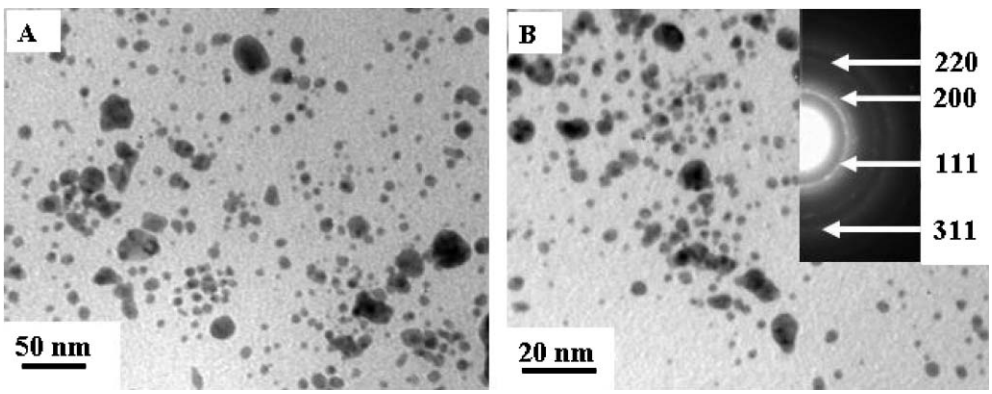

Fig. 3 (A, B) Representative TEM micrographs obtained from the drop-coated films of Au–Ag alloy nanoparticles obtained from the 3Au : 1Ag mixture. The SAED pattern of the Au–Ag nanoparticles is shown in the inset of B.

measurements were carried out on the initial CATB : 3Au : 1Ag solution mixture (prepared by mixing 25 ml each of 3×10^{-3} M $HAuCl_4$ and 1×10^{-3} M Ag_2SO_4 with 50 ml of 2×10^{-2} M solution of CTAB) and then on a sample obtained from dry foam just before the reduction was carried out and after all the excess liquid has been removed. In the solution the ratio of Au : Ag ions was ~3 : 1, very close to the concentration ratio of the ions used in the mixture. However, in the foam after the drainage the ratio of Au : Ag ions is ~8.5 : 1 clearly showing that CTAB selectively binds to $AuCl_4^-$ ions. Then any reduction of this foam matrix would only lead to the formation of gold nanoparticles as observed. In contrast when we use the BSA as foaming material the ratios of Au : Ag ions as determined by AAS analyses in the solution (prepared by taking 25 ml each of 3×10^{-3} M $HAuCl_4$ and 1×10^{-3} M Ag_2SO_4 aqueous solutions and mixed with 50 ml of 3 mg ml^{-1} BSA–water) and from the foam sample (after all the excess liquid was drained out) are ~2.8 : 1 and ~3.3 : 1, respectively. Thus this exercise clearly demonstrates that BSA binds equally well with both the ions and in the foam matrix there is substantial concentration of these two ions that facilitates the alloy formation.

To probe the nature of binding of BSA with both Ag^+ and $AuCl_4^-$ ions in foams in a little more detailed manner, FTIR measurements on the foam samples of BSA with these two ions individually and with their 3 : 1 molar mixture were carried out. The samples were collected from dry foams as has been described above for the AAS measurements and in the Experimental section. In Fig. 4, curve 1 depicts the spectrum of pure BSA, curve 2 is that of a foam sample of BSA with $AuCl_4^-$ ions, curve 3 is that of BSA with Ag^+ ions in foam and curve 4 is the sample taken from a dry foam generated from a 3 : 1 molar mixture of $AuCl_4^-$: Ag^+ with BSA. All these foam samples were generated at the pI of the BSA. In the foam it is expected that Ag^+ ions will be interacting with the carboxylic

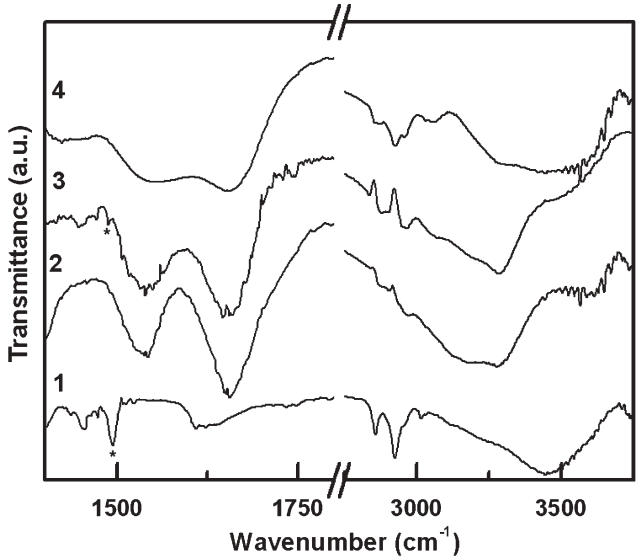

Fig. 4 FTIR spectra in the regions 1400–1800 cm^{-1} and 2750–3750 cm^{-1}, from pure BSA (curve 1), from foam sample of BSA with $AuCl_4^-$ ions (curve 2), BSA with Ag^+ ions in foam (curve 3) and from a foam sample of 3 : 1 molar mixture of $AuCl_4^-$: Ag^+ with BSA.

acid moieties through the formation of carboxylates, while $AuCl_4^-$ ions will be binding to the protonated amine groups. Therefore we expect to see changes in FTIR vibrational frequencies corresponding to these groups. Considering the complexity of the protein structures and the number of amino acids and amide groups they possess it may be very difficult to see drastic changes in the spectra between the free protein and protein interacting with ions as only the carboxylic acids and amines are expected to interact with the ions and the amides do not have much interaction with them. Therefore in the spectra we focus on the regions where we can see some major changes and thus highlight the spectra in the 1400–1800 cm^{-1} and 2750–3750 cm^{-1} regions, which are more pertinent to the discussion here. In the free BSA (Fig. 4, curve 1) the –OH stretching frequency stemming from the free carboxylic acid groups can be seen as a broad peak centered around 3450 cm^{-1}. The –NH asymmetric and symmetric stretching frequencies from $–NH_2$ are also expected around 3400–3500 cm^{-1} regions, but are a little weaker than the –OH stretching frequencies and thus are probably masked. In the spectrum with $AuCl_4^-$ ions (curve 2), we can see a broad peak in the region 3500–3650 cm^{-1}, probably corresponding to the –OH stretching, while peaks from the –NH symmetric and anti-symmetric stretching peaks occur at ~3280 cm^{-1} as well as around 3170 cm^{-1}. Here the former could be coming from the free $–NH_2$ groups not bound to the $AuCl_4^-$ ions, the latter are probably from the amide groups. In curve 3, which is obtained from the foam sample of BSA with Ag^+ ions, the peaks above 3200 cm^{-1} are of very weak intensity and a clear peak emerges at around 3180 cm^{-1}. The intensity loss above 3200 cm^{-1} could be attributed to the formation of carboxylates as they are bonded with Ag^+ ions and the absence of free carboxylic acids. The peak at 3200 cm^{-1} is then ascribed to the $–NH_2$ stretching vibrations of free amine groups as well as those from the amide groups as no interaction is expected between them and the Ag^+ ions. Curve 4 is from the sample where both $AuCl_4^-$ ions as well as Ag^+ ions are present in the BSA foam matrix. Therefore it looks more like an overlapped spectrum of curves 2 and 3 especially in the 3200–3600 cm^{-1} regions. Though we expect a complete absence of free amine and carboxylic acid groups and therefore no peaks in this region if the BSA foam were completely saturated with both Ag^+ and $AuCl_4^-$ ions this may not be the case and probably the presence of some free amine and carboxylic acid groups that are not bound to these ions are responsible for these peaks. The next discernible changes occur in the region 1480–1500 cm^{-1}, which is ascribed to the –NH bending vibrations and the formation of $–NH_3^+$ groups.[22] In curve 1 from pure BSA this can be found at 1494 cm^{-1} (denoted by an asterisk). This band is almost invisible in the BSA–$AuCl_4^-$ sample (curve 2) indicating the formation of a $–NH_3^+$–$AuCl_4^-$ complex. It appears as a weak feature in the BSA–Ag^+ sample (curve 3, denoted by an asterisk) again supporting our contention that there is probably no interaction between the Ag^+ and $–NH_2$ groups. This peak is absent in the BSA–Ag^+–$AuCl_4^-$ sample. This is expected as here again we anticipate that the $–NH_3^+$ groups would be complexing with $AuCl_4^-$ ions. It is worth noting that we do not see major changes in the 1500–1700 cm^{-1} region corresponding to the

carbonyl stretching frequencies though major changes are generally observed between the carboxylic acid and carboxylate ions in this regions. It may be possible that these changes are masked by the amide 1 and amide 2 features of the protein that occur in the 1500–1600 cm^{-1} and 1600–1700 cm^{-1} regions respectively, as there will be innumerable amide bonds present in the protein.

In the second control experiment we did the reduction on $AuCl_4^-$: Ag^+ ions in a BSA solution mixture *i.e.* without forming the foam again by keeping the molar ratios of Au : Ag ions as 3 : 1. In this case the optical spectrum clearly displayed two distinct peaks ascribed to separate Ag and Au nanoparticles in solution apart from a small contribution from the alloy phase (see ESI,† Fig. S2). This again establishes that foaming is an essential step to get the alloy nanoparticles, which makes sure that the reduction occurs on silver and gold ions only bound to the BSA and not with separate ions in solution. Thus, these control experiments clearly exemplify the significance of using BSA and the foaming procedure to get the alloy nanoparticles.

In conclusion, the unique properties of the protein BSA, namely, foaming ability and zwitterionic character at the protein isoelectric point, have been exploited not only to make individual nanoparticle dispersions of Au and Ag with the same foaming surfactant but also to prepare their alloy nanoparticles. This is made possible by carrying ions having opposite charges into the foam column simultaneously and by reducing them *in situ* leading to synthesis of alloy nanoparticles. The resulting nanoparticles are coated/stabilized by the protein molecules and may be eventually be utilized for various biomedical applications.[18]

Acknowledgements

This work was funded by DST to set up a Unit on Nano Science and Technology (DST-UNANST) at NCL and is gratefully acknowledged. We thank Mrs Renu Pasricha, Center for Materials Characterization (CMC), for assistance with the TEM measurements.

References

1 (*a*) *Nanoscale Materials in chemistry*, ed. K. J. Klabunde, Wiley, New York, 2002, p. 1; (*b*) *Science*, 2000, **290**, 1523 (Special Issue on Nanotechnology).
2 (*a*) N. Majeti and V. R. Kumar, *J. Pharm. Pharm. Sci.*, 2000, **3**, 234; (*b*) M. E. Akerman, W. C. Chan, P. Laakkonen, S. N. Bhatia and E. Ruoslahti, *Proc. Natl. Acad. Sci. USA*, 2002, **99**, 12617; (*c*) O. V. Salata, *J. Nanobiotechnol.*, 2004, **2**, 1; (*d*) R. Moller, A. Csaki, J. M. Kohler and W. Fritzche, *Nucleic Acids Res.*, 2000, **28**, e91(1–5); (*e*) T. Liu, J. Tang and L. Jiang, *Biochem. Biophys. Res. Commun.*, 2004, **313**, 3; (*f*) C. Woffendin, Z. Yang, Xu. L. Udaykumar, N. Yang, M. J. Sheehy and G. J. Nabel, *Proc. Natl. Acad. Sci. USA*, 1994, **91**, 11581; (*g*) C. M. Niemeyer, *Angew. Chem., Int. Ed.*, 2001, **40**, 4128; (*h*) A. Bielinska, J. D. Eichman, I. Lee, J. R. Baker Jr. and L. Balogh, *J. Nanopart. Res.*, 2002, **4**, 395; (*i*) H. Nakao, H. Shiigi, Y. Yamamoto, S. Tokonami, T. Nagaoka, S. Sugiyama and T. Ohtani, *Nano Lett.*, 2003, **3**, 1391.
3 M. Sastry, A. Swami, S. Mandal and PR. Selvakannan, *J. Mater. Chem.*, 2005, **15**, 3161.
4 (*a*) *Optical Properties of Metal Clusters*, ed. U. Kreibig and M. Vollmer, Springer, Berlin, 1995; (*b*) P. Mulvaney, *Langmuir*, 1996, **12**, 788.
5 (*a*) J. Schwank, *Gold Bull.*, 1983, **16**, 103; (*b*) N. Toshima, M. Harada, Y. Yamazaki and K. Asakura, *J. Phys. Chem.*, 1992, **96**, 9927; (*c*) M. Harada, K. Asakura, Y. Ueki and N. Toshima, *J. Phys. Chem.*, 1992, **96**, 9730; (*d*) H. Liu, G. Mao and S. Meng, *J. Mol. Catal.*, 1992, **74**, 275.
6 (*a*) P. Mulvaney, M. Giersig and A. Henglein, *J. Phys. Chem.*, 1993, **97**, 7061; (*b*) L. M. Liz-Marzan and A. P. Philipse, *J. Phys. Chem.*, 1995, **99**, 15120; (*c*) B. K. Teo, K. Keating and Y.-H. Kao, *J. Am. Chem. Soc.*, 1987, **109**, 3494; (*d*) J. Sinzig, U. Radtke, M. Quinten and U. Kreibig, *Z. Phys. D*, 1993, **26**, 242; (*e*) N. Kometani, M. Tsubonishi, T. Fujita, K. Asami and Y. Yonezawa, *Langmuir*, 2001, **17**, 578; (*f*) S. Link, Z. L. Wang and M. A. El-Sayed, *J. Phys. Chem. B*, 1999, **103**, 3529; (*g*) J. Turkevich, P. C. Stevenson and J. Hillier, *Discuss. Faraday Soc.*, 1951, **11**, 55; (*h*) D. Chen and C. J. Chen, *J. Mater. Chem.*, 2002, **12**, 1557; (*i*) I. Lee, S. Han and K. Kim, *Chem. Commun.*, 2001, 1782; (*j*) G. C. Papavassiliou, *J. Phys. F: Met. Phys.*, 1976, **6**, L103; (*k*) T. Sato, S. Kuroda, A. Takami, Y. Yonezawa and H. Hada, *Appl. Organomet. Chem.*, 1991, **5**, 261.
7 (*a*) *Colloids and Colloid Assemblies*, ed. F. Caruso and M. Sastry, Wiley-VCH, Weinheim, 2004, p. 369; (*b*) A. Swami, P. R. Selvakannan, R. Pasricha and M. Sastry, *J. Phys. Chem. B*, 2004, **108**, 19269; (*c*) S. S. Shankar, D. Rautaray, R. Pasricha, N. R. Pavaskar, A. B. Mandale and M. Sastry, *J. Mater. Chem.*, 2003, **13**, 1108; (*d*) C. Damle and M. Sastry, *J. Mater. Chem.*, 2002, **12**, 1860.
8 *Physics of Foams*, ed. D. Weaire and S. Hutzler, Oxford University Press, Oxford, 1999.
9 B. D. Dong, J. J. Cilliers, R. J. Davey, J. Garside and E. T. Woodburn, *J. Am. Chem. Soc.*, 1998, **120**, 1625.
10 (*a*) S. Mandal, S. K. Arumugam, S. D. Adyanthaya and M. Sastry, *J. Mater. Chem.*, 2004, **14**, 43; (*b*) T. Bala, S. Arumugham, R. Pasricha, B. L. V. Prasad and M. Sastry, *J. Mater. Chem.*, 2004, **14**, 1057; (*c*) T. Bala, S. D. Bhame, P. A. Joy, B. L. V. Prasad and M. Sastry, *J. Mater. Chem.*, 2004, **14**, 2941.
11 D. Rautray, K. Sinha, S. S. Shankar, S. D. Adyanthaya and M. Sastry, *Chem. Mater.*, 2004, **16**, 1356.
12 S. S. Shankar, U. Patil, B. L. V. Prasad and M. Sastry, *Langmuir*, 2004, **20**, 8853.
13 X. L. Huang, G. L. Catignani and H. E. Swaisgood, *J. Food Sci.*, 1997, **62**, 1028.
14 (*a*) W. C. Thuman, A. G. Brown and J. W. McBain, *J. Am. Chem. Soc.*, 1949, **71**, 3129; (*b*) S. H. Richert, *J. Agric. Food Chem.*, 1979, **27**, 665; (*c*) P. N. Peter and R. W. Bell, *Ind. Eng. Chem.*, 1930, **22**, 1124; (*d*) S. Damodaran, K. Anand and L. Razumovsky, *J. Agric. Food Chem.*, 1998, **46**, 872.
15 Please see http://www-biol.paisley.ac.uk/Courses/Enzymes/glossary/Foaming.htm.
16 (*a*) A. Kumar, M. Pattarkine, M. B. Bhadbhade, A. B. Mandale, K. N. Ganesh, S. S. Datar, C. V. Dharmadhikari and M. Sastry, *Adv. Mater.*, 2001, **13**, 341; (*b*) M. Sastry, A. Kumar, S. S. Datar, C. V. Dharmadhikari and K. N. Ganesh, *Appl. Phys. Lett.*, 2001, **78**, 2943; (*c*) W. Shenton, T. Douglas, M. Young, G. Stubbs and S. Mann, *Adv. Mater.*, 1999, **11**, 253; (*d*) J. L. Turner, M. L. Becker, X. Li, J. A. Taylor and K. L. Wooley, *Soft Matter*, 2005, **1**, 69.
17 (*a*) R. Shenhar and V. M. Rotello, *Acc. Chem. Res.*, 2003, **36**, 549; (*b*) F. Caruso, *Adv. Mater.*, 2001, **13**, 11; (*c*) J. Park, W. Lee, S. Bae, Y. J. Kim, K. Yoo, J. Cheon and S. Kim, *J. Phys. Chem. B*, 2005, **109**, 13119; (*d*) B. L. Frankamp, O. Uzun, F. IIhan, A. K. Boal and V. M. Rotello, *J. Am. Chem. Soc.*, 2002, **124**, 892; (*e*) J. Kolny, A. Kornowski and H. Weller, *Nano Lett.*, 2002, **2**, 361.
18 (*a*) A. M. Derfus, W. C. W. Chan and S. N. Bhatia, *Adv. Mater.*, 2004, **16**, 961; (*b*) M. Mikhaylova, D. K. Kim, C. C. Berry, A. Zagorodni, M. Toprak, A. S. G. Curtis and M. Muhammed, *Chem. Mater.*, 2004, **16**, 2344.
19 The serum albumin protein structure was retrieved from the Protein Data Bank (URL: http://www.rcsb.org/pdb/). The ID No. was IA06.
20 (*a*) S. Link and M. A. El-Sayed, *J. Phys. Chem. B*, 1999, **103**, 4212; (*b*) K. L. Kelly, E. Coronado, L. L. Zhao and G. C. Schatz, *J. Phys. Chem. B*, 2003, **107**, 668.
21 *Electro Deposition of Alloys: Principles and Practice*, ed. A. Brenner, Academic Press, New York, vol. 1, 1963.
22 (*a*) S. Choudhury, PhD Thesis, University of Pune, India, 1995; (*b*) M. Bardosova, R. H. Tredgold and Z. Ali-Adib, *Langmuir*, 1996, **11**, 1273.